World Conference on
Timber Engineering
Oslo 2023

POINT-SUPPORT REINFORCEMENT FOR A HIGHLY EFFICIENT TIMBER HOLLOW CORE SLAB SYSTEM

Cristóbal Tapia[1], Hans Jakob Wagner[2], Simon Treml[3], Achim Menges[4], Simon Aicher[5]

ABSTRACT: The paper presents a new point-supported slab building system concept developed at the Cluster of Excellence on Integrative Computational Design and Construction for Architecture (IntCDC) at the University of Stuttgart. The system uses a hollow-core system with two thin CLT plates acting as flanges and a set of distributed shear web elements in-between. The introduction of point supports induces large shear forces concentrated in the narrow region surrounding the column. This area is reinforced by an LVL core placed in-between CLT flanges, at the column-head position, with discrete web elements connected laterally to introduce the shear forces. Two alternative solutions for this connection are presented, differing mainly in the chosen strategy to bond both components: side bonding of web beams into the LVL core, or only gluing the frontal sloped face of the web beams. An experimental campaign was set, where a total of three specimens of each alternative where manufactured and tested. The results showed a clear superiority of the side-bonded web beams, reaching capacities between four to five times larger than the alternative without side bonding. The paper discusses the relationship of the system with robotic manufacturing processes and presents experimental and corresponding finite element results.

KEYWORDS: multi-storey timber buildings, CLT, LVL, beech LVL, web beam bonding, robotic manufacturing, hybrid composite

1 INTRODUCTION

The last decade has seen a steady increase of multi-storey timber projects [2, 9, 14, 16] enabled by the continuous development of new technologies, including novel connections and structural elements (see e.g. [10, 22]). This trend will foreseeable continue during the next years, as it allows for an efficient use of the already scarce construction area in cities, while offering incentives to reduce CO_2 emissions and improve construction conditions (less noise and shorter build times). Thus, timber is becoming a viable alternative to the presently dominant reinforced concrete (RC) building systems. This is at least true for multi-storey building typologies that afford rigid grids and single span structural systems [16]. However, to achieve similar capabilities as with reinforced concrete or steel buildings in terms of architectural flexibility and long-term (re)-usability, timber-based construction systems must be further developed to increase the possibilities and design freedom of the (re-) distribution and (re-) partitioning of inner spaces. This typically requires relatively long spans, a limited amount of columns that can be freely positioned to optimize flexible use-options and a flat bottom side of the slab to simplify the reinstallation of spatial divisions (inner walls).

Applied to timber structures, such a flexible point-supported slab structure presents several challenges. For example, this concept presupposes a biaxial mechanical behavior of the plate elements, which for the case of timber requires special considerations on the level of edge connections, as plate dimensions are limited by production and transport constraints. Then, since the whole floor plan acts as a monolithic, biaxial plate, large and rather concentrated negative moments form in the immediate proximity and directly above each column, which adds to the high shear stresses in the same region.

These problems constituted important research topics in the last years, where the focus has been placed mainly on the use of cross-laminated timber (CLT) plates. These efforts have lead to the development of several connection concepts for point-supported CLT plates [10, 11, 18, 22], as well as stiff edge connections for CLT plates [3, 17]. Both of these concepts are essential to achieve a slab system with biaxial mechanical behavior, large spans and a flexible arrangement of columns.

However, in terms of material efficiency, the use of CLT

[1]Materials Testing Institute (MPA), University of Stuttgart, Pfaffenwaldring 4b, 70569 Stuttgart, Germany, cristobal.tapia-camu@mpa.uni-stuttgart.de
[2]Institute for Computational Design and Construction (ICD), University of Stuttgart, Keplerstraße 11, 70174 Stuttgart, Germany, hans.jakob.wagner@icd.uni-stuttgart.de
[3]Institute for Computational Design and Construction (ICD), University of Stuttgart, Keplerstraße 11, 70174 Stuttgart, Germany, simon.treml@icd.uni-stuttgart.de
[4]Institute for Computational Design and Construction (ICD), University of Stuttgart, Keplerstraße 11, 70174 Stuttgart, Germany, achim.menges@icd.uni-stuttgart.de
[5]Materials Testing Institute (MPA), University of Stuttgart, Pfaffenwaldring 4b, 70569 Stuttgart, Germany, simon.aicher@mpa.uni-stuttgart.de

https://doi.org/10.52202/069179-0388

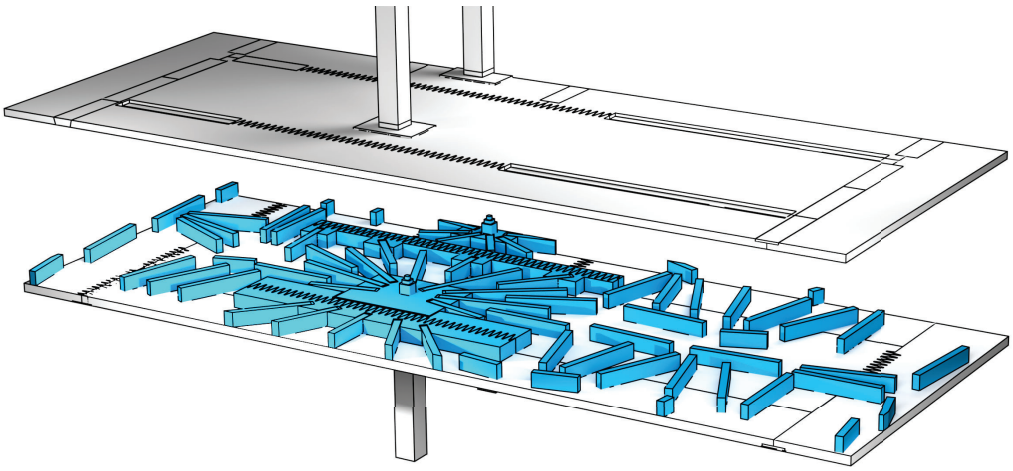

Figure 1: *Illustration of the development of a new hollow-core slab building system based on CLT outer plates with discrete distributed GLT web elements*

for large spans can be regarded as rather wasteful compared to different, more optimized systems. For example, the slab elements used in the building "Mjøstårnet", Norway, were conceived as ribbed elements, thus making a more efficient use of the material [2]. The general concept of ribbed slab elements is appealing in many ways, however, the current implementations—mostly devised as unidirectional elements—restrict the layout of columns to rather strict rectangular grids. Hence, the design space is severely limited [16]. Concepts also exist for computationally designed reinforcing beam networks of timber slabs for flexible column positions [4]. Several questions regarding its structural performance and fire-resistance are not yet answered and in the immediate future this approach seems not economically viable for large-scale building structures.

At the Cluster of Excellence on Integrated Computational Design and Construction for Architecture (IntCDC) of the University of Stuttgart a new slab building system concept is currently being investigated that aims to overcome design limitations of conventional systems in an economically viable manner. This timber building system is conceptualized as a point supported flat slab for large and multi-directional spans without the use of steel and concrete details. An early iteration of the system was presented in [8, 13]. The general concept consists of a hollow-core system with two rather thin CLT plates acting as flanges and a set of discrete, optimally distributed shear web elements in-between. Such a system is naturally very efficient for long spans, however, the introduction of point supports presents demanding challenges, as large shear forces concentrate in one narrow region. Due to the hollow nature of the slab, not enough material is present to resist the highly concentrated shear forces, thus requiring a special solution to reinforce the plate in the region of the supports.

This contribution presents the current development state of a hybrid hard- and softwood solution for the reinforcement of the highly stressed region above the point-supports of a hollow-core slab system. Important aspects of the interrelationship of the system with robotic manufacturing processes are discussed, and first experimental and corresponding finite element results are presented. Finally, the possibilities and limitations for practical applications of the system will be discussed.

2 DESCRIPTION OF THE SYSTEM

2.1 GENERAL

The slab system is composed of two CLT plates acting as biaxial *flanges* and a set of relatively short GLT elements glued between both CLT plates, which take the role of web elements (see Fig. 1). The exact position and orientation of these web elements varies throughout the extension of the floor and is determined by an agent-based model that considers the field of shear forces computed by a finite element (FE) model of the analyzed building [12]. In essence, the web elements are oriented following the shear force trajectories, thus aiming at an efficient utilization of the material. The described build-up of the slab system enables a biaxial behavior with very similar bending stiffness in both principal axes. Depending on the floor plan of the building, the column positions and applied set of loads, regions of high or low *density* of these web elements arise.

2.2 ROBOTIC MANUFACTURING CONCEPT

This differentiated distribution of shear webs within the hollow slab is further enabled by a robotic assembly process of the hollow slab elements. The exact position data of the webs from the computational design methods mentioned above can be directly streamed to a robotic fabrication platform, that assembles the web elements in their exact position. This process was tested for a small scale project presented in [15]. As the robotic platform is digitally controlled the complexity of assembling webs in unique patterns is the same as assembling the webs in standardized positions. Hence the co-design of the slab with optimized web layouts together with digital manufacturing processes allows for optimization potentials in the slab that would be not feasible without the integration of digital design and

https://doi.org/10.52202/069179-0388

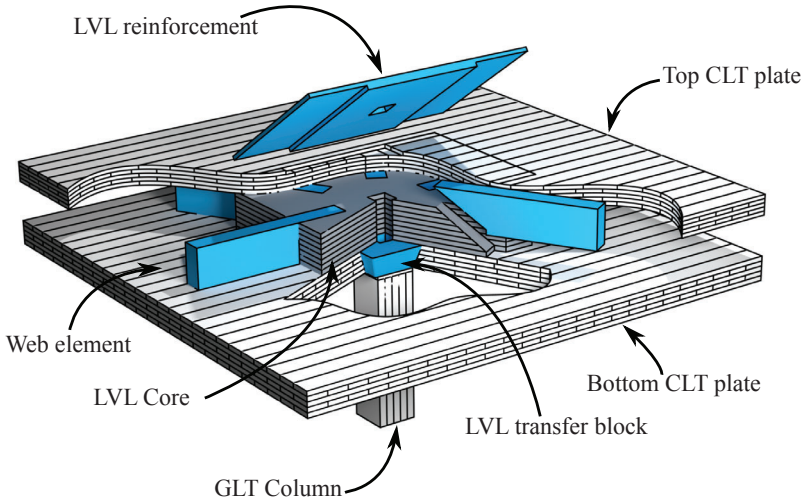

Figure 2: *Concept point-supported hollow-core plate system*

robotic fabrication. The robotic fabrication process nevertheless also has reciprocal requirements to be considered in the internal structural details of the slab. This is especially relevant regarding the structural connection of webs to upper and lower flange and their connection to reinforcement elements inside the hollow slab. The fabrication concept envisions that the robot first selectively applies adhesive on the bottom plate in all areas where webs will be placed. Subsequently webs are placed on the adhesives and pressed with partially-threaded screws. After curing of the bond line between bottom plate and web beams and removal of screws, the plate arrives again at the robotic fabrication setup. Adhesive is applied on top of the webs and the top plate is placed and pressed again using screws. Through this process a structural bond of the inner elements with upper and lower plate can be established completely independent of hydraulic, mechanical or vacuum cramping equipment.

2.3 STRUCUTRAL CHALLENGES AROUND COLUMN SUPPORTS

Intuitively, regions of higher positive moments towards the center of the spanned fields are subject to lower shear forces, thus reducing the density of web elements. On the other side of the spectrum, in the regions surrounding a column the sectional shear forces rapidly increase, requiring a higher amount of material (more webs). Furthermore, the same region will be subjected to highly concentrated negative moments, imposing high biaxial tensile stresses in the plane of the top CLT plate. This is further worsened by the typical presence of a hole, necessary for the transfer of vertical column loads originating in the upper floors of a multi-storey building (see e.g. [10, 14]).

In order to safely handle these unfavorable stresses, a special reinforcement concept is needed. Such concept must consider both, the shear forces and the tensile stresses in the top plate. A possible solution for this is shown in the following.

2.4 COLUMN-HEAD CONCEPT

The proposed solution is composed of three elements, which are illustrated in Fig. 2. Starting from top to bottom the following components are present: (i) an LVL plate on the upper side of the top CLT plate to take care of the reinforcement against high tensile stresses due to negative moments; (ii) a solid LVL block with cavities for the attachment of incoming web elements to help resisting the high shear forces; and (iii) a smaller LVL block inserted in the bottom CLT plate, directly above the column head, to reinforce against failure due to high shear and compressive stresses. These three components are glued to the CLT plates to ensure an efficient load and stress transmission.

The plate for the reinforcement of tensile stresses is the same as presented in [18] for a reinforcement concept for CLT plates, and is therefore not discussed in detail in this paper. The main topic of this paper is the LVL block for the reinforcement of shear forces, where different aspects related to the manufacturing and structural efficiency are covered.

The relatively high shear strength of the spruce LVL block—compared to typical softwood CLT—allows to resists the high shear forces in the region surrounding the column. These forces are mainly coming from the web elements, which raises the question regarding the connection between webs and LVL block.

For the ease of robotic fabrication it would be preferred if a lateral connection between shear web and LVL reinforcement can be avoided. However, for heavily loaded columns this would increase the necessary dimension of the LVL block, as enough surface is required to transfer the shear stresses. In this paper, two alternatives are investigated, resulting from the manufacturing constraints discussed above.

https://doi.org/10.52202/069179-0388

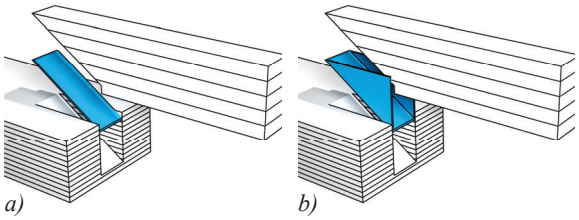

Figure 3: *Alternatives investigated for the application of the adhesive in the connection between GLT web and LVL core elements; (a) Alternative A; (b) Alternative B*

2.5 ALTERNATIVES FOR CONNECTION BETWEEN LVL CORE AND WEB ELEMENTS

2.5.1 Alternative A

The alternative A considers the milling of a wedge-shaped cavity with angle α in the LVL block with a width $w_b > w_w$, where $w_w = 100\,\text{mm}$ is the width of the web element (see Fig. 3a). The end of the web is cut with the same angle α as present in the LVL block. Relatively high tolerances in the horizontal plane need to be considered when large wooden elements are fully robotically assembled. This stems from several factors such as inconsistent dimensional accuracy of GLT beams, manufacturing tolerances of cavity and positioning accuracy of the robotic placement. Between the lateral faces of the GLT and LVL elements a gap with thickness $t_A = 10\,\text{mm}$ is left. This enables a robust robotic placement of the webs into the cavities.

The inclined surface of the web needs to be bonded with the inclined surface of the LVL block. The adhesive that can be applied by the robotic fabrication platform is partially gap-filling up to bond line thicknesses of 1.5 mm. This demands a highly accurate positioning of the web in direction of the longitudinal axis of the web. For this requirement a *locator feature* (see Fig. 4) was included in the web and LVL block geometry, which enables the robot to press the web laterally against the LVL block to ensure precise positioning. Subsequently, the adhesive interfaces between web-bottom plate and web-LVL block are pressed via screws. Further small pockets were included in the design of the LVL cavity and web geometry, to avoid that cured adhesives overruns restrict neither the correct positioning of the web nor that of the top plate.

2.5.2 Alternative B

Alternative B considers a three-sided embedment of the web beam end in the LVL block (see Fig. 3b). This is done by filling the lateral cavities between the LVL block and web beam with a gap-filling, two-component epoxy adhesive, enabling the transfer of shear stresses through these surfaces. From a mechanical perspective, this should be more efficient than alternative A, as more surface is available for the transfer of stresses, and on the side of the web element the surfaces are aligned with the main axis of the GLT element. Compared to alternative A, the gap must be smaller, to avoid using too much adhesive, leading to possible extreme exothermic reactions. Therefore, the gap is set to $t_B = 3\,\text{mm}$. For the fabrication of Alternative B the placement of the web can be achieved within the typical tolerances. Nevertheless, the filling of the gap with the two-component adhesive is a rather laborious task for an automated process. This is mainly because the gap between web and LVL needs to be sealed before glue application, then the glue needs to be filled without impacting the quality of the top web and LVL surface. Finally, the robotic fabrication platform considered for the fabrication of the hollow slab components is not equipped with a two-component epoxy application system. Hence, the fabrication concept for Alternative B considers the robotic placing the web beam into the LVL block, but bonding is performed exclusively to the bottom CLT plate. While the adhesive interfaces between inner elements and bottom plate are stored for curing, the gap between LVL block and web is manually filled with the two-component epoxy adhesive.

3 EXPERIMENTAL CONFIGURATIONS AND MANUFACTURING

3.1 STUDIED CONFIGURATIONS

The shear capacity of the connection was experimentally investigated for both alternatives A and B. The angle α was varied such that the side ratio $r_\alpha = \arctan(\alpha) = 1{:}1$, 1:1.5 and 1:2. The experimental set-up is illustrated in Fig. 5. Here, the LVL core is clamped by pressing a steel plate on the top of the LVL core to a steel I-beam on the bottom by tightening one full-threaded rod at each side. Below the LVL core a set of steel plates were arranged, such that only the area directly below the embedded web beam was allowed to rotate freely (see Fig. 5). The load was applied on a steel plate placed on the top face of the GLT web, at a distance of 20 mm from the edge of the LVL core. The total length of the loading plate varied for each configuration, being $\ell_s = 100\,\text{mm}$ for $r_\alpha = 1{:}1$ and $\ell_s = 220\,\text{mm}$ for $r_\alpha = 1{:}1.5$ and 1:2, respectively.

Self-tapping screws were inserted directly under the loading plate to reinforce this region and to better distribute the shear stresses within the cross-section.

The specimens were tested at the Division of Timber Constructions of the Materials Testing Institute, University of Stuttgart, with a servo-hydraulic universal testing machine with a maximum load capacity of 1.6 MN. The load was applied in displacement-controlled manner with a stroke rate of 0.1 mm/min.

3.2 PROTOTYPE MANUFACTURING

The LVL core was manufactured by bonding six layers of unidirectional spruce LVL plates, where each plate was oriented orthogonally with respect to the adjacent plates. The top-most plate is oriented in the direction parallel to the GLT's main axis. On each LVL block two inclined cavities were milled at the opposite sides, parallel to the main axis of the experimental set-up. This enabled to test connection alternative A on one side and alternative B on the opposite side independently. The cavities in the LVL block were milled with a Kuka Industrial Robot at Züblin Timber GmbH, Aichach, Germany.

https://doi.org/10.52202/069179-0388

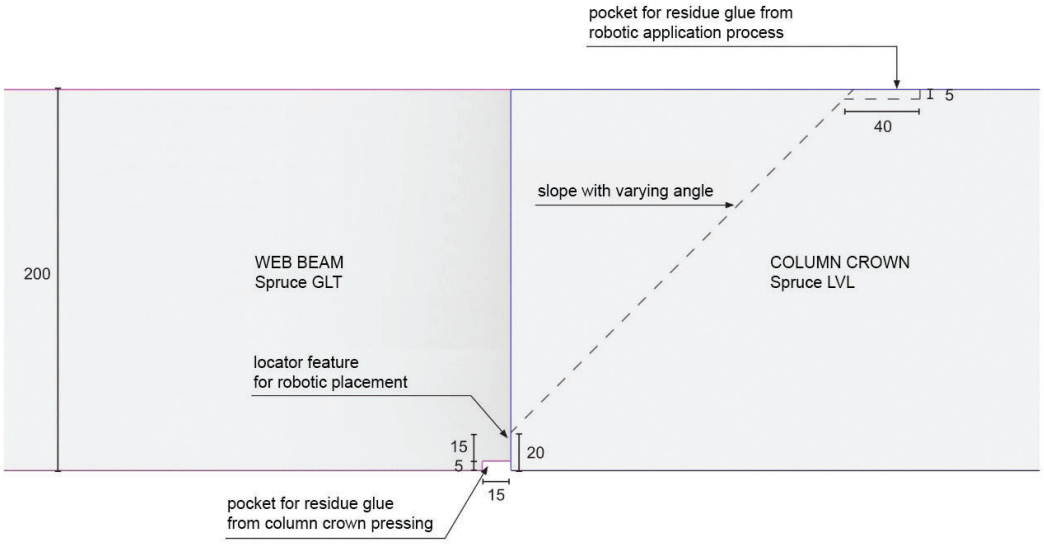

Figure 4: *Locator feature and pockets for residue glue in Alternative A for precise robotic placement*

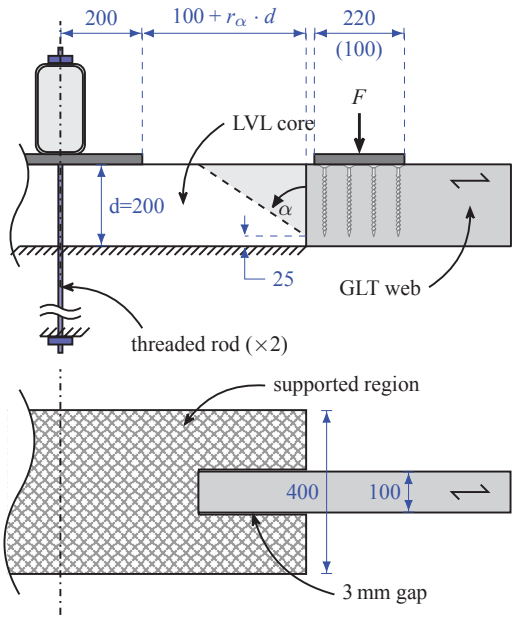

Figure 5: *Experimental set-up used for the study of both alternatives A and B*

Figure 6: *Realized experimental setup*

3.3 BONDING OF SPECIMENS

The bonding of alternative A was performed by applying an aminoplastic melamine-urea-formaldehyde (MUF) adhesive directly on the inclined surfaces of both, the GLT and LVL elements, and then evenly spreading the adhesive with a spatula. Hereinafter, the GLT beam was placed in its intended position, followed by the insertion of two to four partially threaded screws (depending on the geometry) to produce the required pressure. One or two screws were placed vertically, while the others were inserted in a direction perpendicular to the inclined surface. A dummy softwood plate, later removed, was placed below the LVL block in order to provide anchoring material for the threaded screw part.

The procedure followed to bond alternative B consisted on securing the GLT element in its position by means of screws and then sealing the vertical gaps between LVL and GLT by means of a special adhesive tape. Thereafter, the two-component epoxy adhesive was injected through predrilled holes until the gap was completely adhesive-filled.

All specimens were left to cure for at least two days before proceeding with the tests.

https://doi.org/10.52202/069179-0388

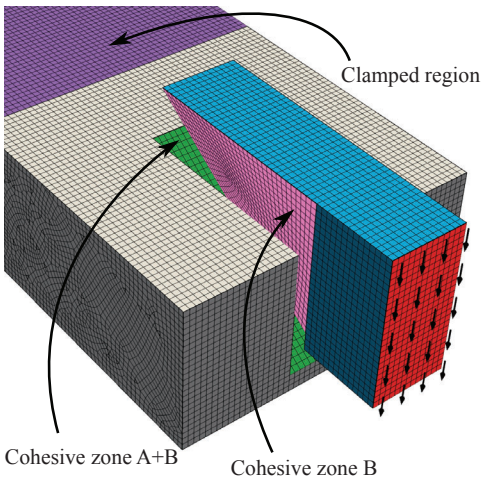

Figure 7: *Geometry, discretization of the implemented finite element model, together with the application of loads and definition of cohesive regions*

4 FINITE ELEMENT MODEL

A 3D finite element (FE) model was implemented with the Python API of the software Abaqus [1]. The model uses linear brick and wedge continuum elements of type C3D8 and C3D6, together with the elastic mechanical properties shown in Table 1. The length of the web beam was defined such that its outer end coincides with the center of the load application point. This reduces the amount of elements in the model and enables the load application in a more evenly distributed manner (see below).

An illustration of the discretization of the model is presented in Fig. 7, where the mesh size is about 20 mm. The bonded interfaces in both alternatives, A and B, were modelled with a cohesive behavior with stiffness parameters $k_n = k_t = 1000\,\mathrm{N/mm^3}$. The cohesive regions used for each alternative are shown in Fig. 7. The clamping condition was simulated by restraining the vertical displacement on a surface at the bottom face, according to Fig. 5, and at the top, while the load application was done by introducing a distributed vertical load on the outer vertical face of the GLT element (see Fig. 7).

The results were saved in the ASCII format (*.fil) and later post-processed with the Python library Pybaqus [19]. The scripts used for this paper are available in [20].

5 EXPERIMENTAL AND NUMERICAL RESULTS

5.1 FEM RESULTS

5.1.1 Shear stresses on the bonded surfaces

The FE model was used to inspect the distribution of shear stresses on the bonded surfaces. Figures 8a and 8b show the shear stresses obtained for $r_\alpha = 1{:}1.5$ for alternatives A and B, respectively. It can be seen that the stresses on alternative B (side bonding) are more evenly distributed and reach lower maximum values than for the case of alternative A. Specifically, the stresses on alternative A reach values about two times higher (see Fig. 9). In general, this

Table 1: *Elastic material stiffness properties used for the FEM simulations*

Material	E_0 * [MPa]	E_{90} [MPa]	ν_{12} [–]	ν_{23} [–]	G [MPa]	G_r [MPa]
CLT[1)]	11 000	370	0.2	0.02	690	50
LVL[2)]	12 800	2000	0.2	0.02	430	43

[1)] acc. to values in [6] for softwood boards strength class C24 as indicated in [7]

[2)] acc. to values in [5, 21] (except ν_{ij})

* E_0: MOE parallel to fiber; E_{90}: MOE perpendicular to fiber; G: shear modulus; G_r: rolling shear modulus; $\nu_{12} = \nu_{13}$: Poisson coefficient between the fiber direction and the other two orthogonal directions; ν_{23} Poisson coefficient between both directions perpendicular to the fiber direction.

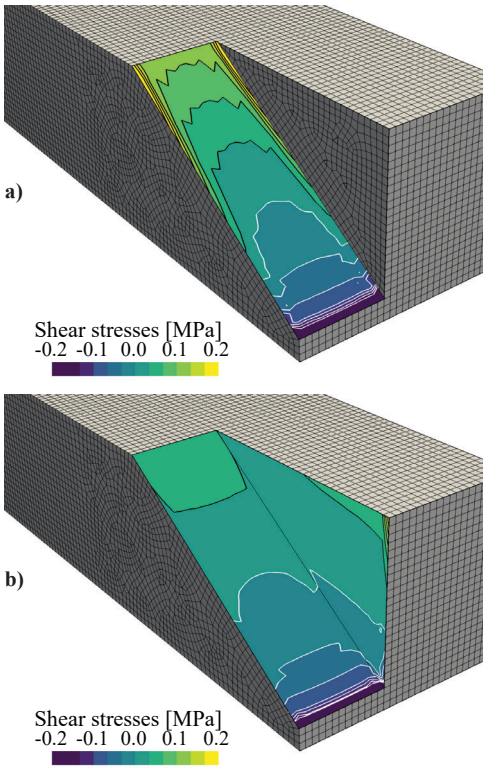

Figure 8: *Shear stresses on the bondfaces for a ratio $r_\alpha = 1{:}1.5$; (a) Alternative A; (b) Alternative B*

is an expected result, which is owed to the larger bond surface of alternative B.

5.2 EXPERIMENTAL RESULTS

5.2.1 General behavior

The general behavior of the tested specimens can be described with the help of Fig. 10a–c, where the load-displacement curves corresponding to the averaged measurements of front and back LVDT's are presented. These LVDT's measure the relative vertical displacement between GLT and LVL elements (see Fig. 6). The load-displacement responses of the specimens of type A presented mostly a perfectly linear behavior until the maximum load was

https://doi.org/10.52202/069179-0388

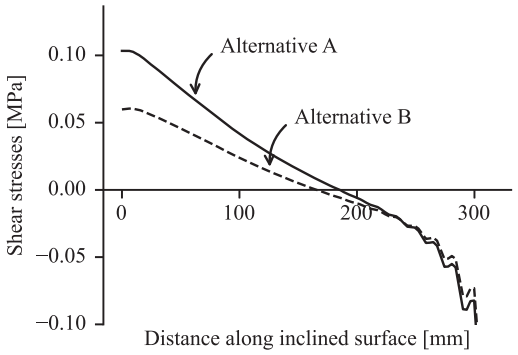

Figure 9: *Shear stresses along the longer dimension of the inclined bonded surface for both alternatives with r_α = 1:1.5 (applied load of* 1 kN*)*

Table 2: *Maximum capacities reached by each specimen*

r_α	Alternative A [kN]	Alternative B [kN]
1:1	20.0	106.1
1:1.5	31.4	122.5
1:2	31.2	119.6

reached, followed by a very brittle failure. The exception was Specimen A-1, which presented a clear stiffness reduction at about 10 kN, thereafter exhibiting a rather nonlinear behavior. The global failure was characterized by the complete de-bonding of the GLT from the LVL element (see Figs. 11a–c).

The behavior of specimens of type B presented a clear nonlinear behavior beyond about 40 % to 50 % of ultimate capacity, then showing a progressively decreasing stiffness for higher loads. The type of post-peak behavior varied for each specimen, where Specimen B-1 (r_α = 1:1) presented the most brittle behavior and Specimen B-3 (r_α = 1:2) showed an almost perfectly plastic behavior. Specimen B-2 (r_α = 1:1.5) lays in-between specimens B-1 and B-3 regarding the post-peak behavior.

Regarding the maximum capacities, Specimens B-2 and B-3 present a similar level ($F \approx 120$ kN), while Specimen B-1 showed a lower value of F = 106 kN. The maximum loads achieved by each specimen are summarized in Table 2. In general, the specimens of type B reached maximum capacities about four to five times larger than specimens of type A. This is an expected results, as the specimens of type B (bonded on the side-faces) not only have a larger bond surface, but also present a more favorable bonding regarding the orientation of the fibers (in type A the fibers are mostly bonded on the end-grain).

5.3 COMPARISON WITH FE RESULTS

The dashed lines in Fig. 10b represent the load-displacement results obtained by the FE model. While a good agreement can be observed for alternative A, the calculated stiffness for alternative B is clearly underestimating the experimental results. This discrepancy might

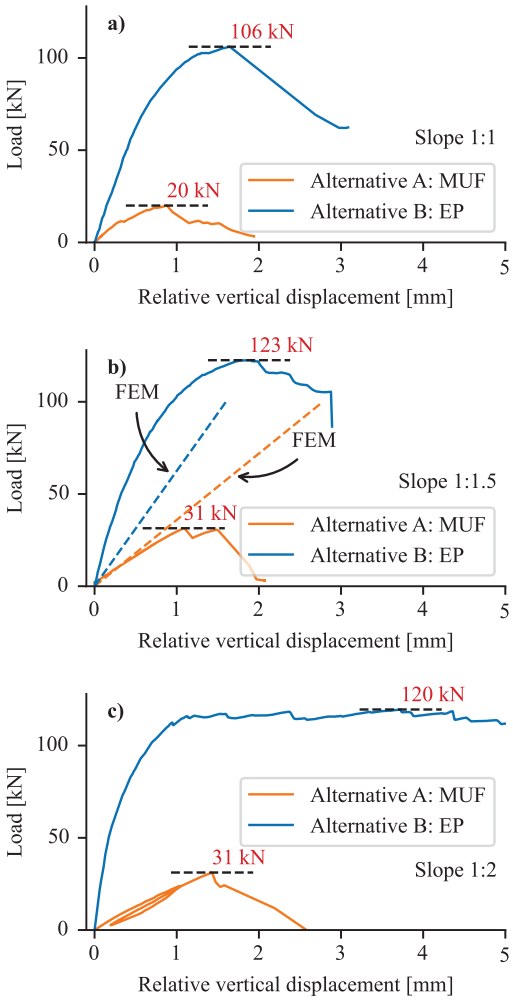

Figure 10: *Load-displacement curves and maximum capacities with data from LVDT's measuring the relative vertical displacement between GLT and LVL for the different investigated alternatives A and B; (a) slope r_α = 1:1; (b) slope r_α = 1:1.5; (c) slope r_α = 1:2*

be explained by the simplification of the load application in the model with respect to the actual load application, as shown in Fig. 5. The numerical corroboration of this effect was left out of this paper due to time constraints.

5.4 ACHIEVED QUALITY OF THE BONDFACES

The bondfaces of the three specimens corresponding to alternative A can be seen in Fig. 11a–c. All surfaces were fully detached immediately after reaching maximum load, as can be suspected from the rather brittle behavior observed. Based on the amount of fiber breakage present, it can be stated that the quality of the bonding was rather poor, as large regions with blunt failures can be seen. This means that the relatively low maximum capacities obtained by the specimens of type A are strongly influenced by the difficulty associated to this kind of bonding.

https://doi.org/10.52202/069179-0388

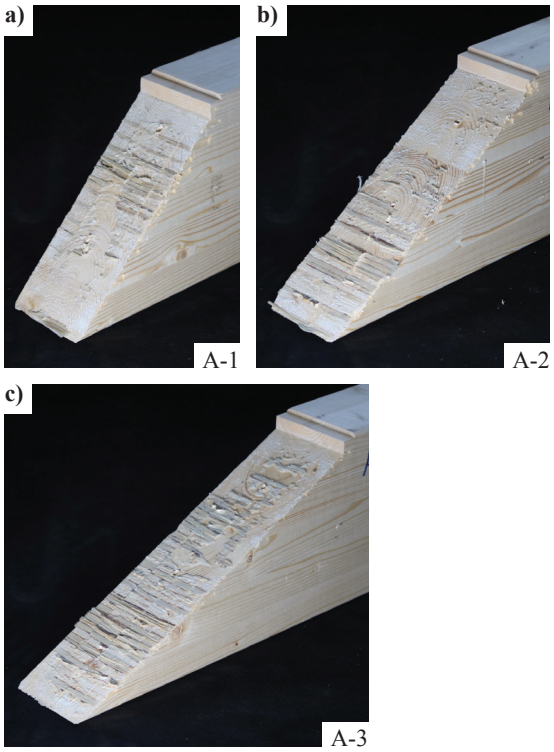

Figure 11: *Bondfaces of specimens of type A after global failure; (a) slope r_α = 1:1; (b) slope r_α = 1:1.5; (c) slope r_α = 1:2*

6 DISCUSSION

6.1 SUITABILITY FOR THE LARGE DEMONSTRATOR BUILDING

Although the connection of type B achieves clearly a better performance than alternative A, the suitability of both alternatives should be assessed based on the requirements for the connection in a real case-study. In this paper, the "Large-Scale Construction Robotics Laboratory" (LCRL)—a building set to apply the different research outputs from the IntCDC Cluster—is used as an example by considering the maximum design loads at the position of the column supports. According to the current state of the design of this building, the column has to resist a maximum design shear force of 753 kN. Considering a total of eight such web elements embedded in a radial pattern around the LVL core element, it is clear that the experimental capacities from alternative A do not reach the needed requirements for the connection. Therefore, alternative B should be preferred in this case.

6.2 GEOMETRY ADJUSTMENTS

Having done the experiments and considering the clearly better results obtained for alternative B, a logical next step is to simplify the connection by removing the inclined bondface altogether. Then, the web would have a typical prismatic shape and would be embedded into the LVL core by means of the same procedure used for alternative B. Experiments to assess this idea are underway and their results will be used to plan a full sized prototype of the slab system.

7 CONCLUSIONS AND OUTLOOK

This paper presented the current state of the slab system developed within the IntCDC Cluster at the University of Stuttgart. In particular, the connection of the shear web elements to the LVL core was investigated by analyzing different geometries and bonding strategies. Based on the experimental and numerical results, as well as on the experience gained from manufacturing the tested specimens, the following conclusions can be stated:

1. The bonding of the lateral faces (alternative B) delivered between four and five times larger maximum capacities in the connection.
2. Based on preliminary design loads for a planned demonstrator building, the rather low capacities exhibited by alternative A do not meet the requirements for the intended use case, thus alternative B should be preferred.
3. The rather low capacities achieved by alternative A, are due to an inferior bonding quality, as could be corroborated in a post-mortem analysis of the specimens.
4. The visualization of the shear stress distribution on the bond faces by means of FE simulations revealed rather uniformly distributed stresses for alternative B, providing additional evidence for the better suitability of side bonded faces for this application.
5. Based on the experimental results, the geometry of the connection will be simplified, removing the inclined surface to increase the lateral bonding surface.

ACKNOWLEDGEMENTS

The presented ongoing research is partially supported by the Deutsche Forschungsgemeinschaft (DFG, German Research Foundation) under Germany's Excellence Strategy – EXC 2120/1 – 390831618. Likewise, the authors would like to thank Thomas Mantzel, Simon Schmid and the team at Züblin Timber (Aichach) for their support.

DATA AVAILABILITY

Some or all data, models, or code generated or used during the study are available in a repository or online in accordance with funder data retention policies. (doi: 10.18419/darus-3381, Ref. [20])

REFERENCES

[1] Abaqus v2020. *ABAQUS/Standard User's Manual, Version 2020*. Providence, RI, USA: Dassault Systèmes, 2020.

[2] R. Abrahamsen. "Mjøstårnet – Construction of an 81 m tall timber building." In: *23. Internationales Holzbau-Forum (IHF)*. Garmisch-Partenkirchen, Germany, 2017.

https://doi.org/10.52202/069179-0388

[3] J. Asselstine, F. Lam, and C. Zhang. "New edge connection technology for cross laminated timber (CLT) floor slabs promoting two-way action." In: *Engineering Structures* 233 (2021), p. 111777. DOI: 10.1016/j.engstruct.2020.111777.

[4] H. Chai, H. J. Wagner, Z. Guo, Y. Qi, A. Menges, and P. F. Yuan. "Computational design and on-site mobile robotic construction of an adaptive reinforcement beam network for cross-laminated timber slab panels." In: *Automation in Construction* 142.August (2022), p. 104536. ISSN: 09265805. DOI: 10.1016/j.autcon.2022.104536.

[5] DOP PM–017–2022. *Pollmeier Furnierwerkstoffe GmbH: Laminated veneer lumber made from beech for non-load bearing, load bearing and stiffening elements – Board BauBuche S and BauBuche Q*. Declaration of Performance. 2022.

[6] EN 338. *Structural timber – Strength classes*. Brussels, Belgium: European Committee for Standardization, 2016.

[7] ETA-06/0009. *Binderholz Brettsperrholz – Massives plattenförmiges Holzbauelement zur Verwendung als tragendes Bauteil in Bauwerken*. European Technical Assessment. Berlin, Germany, 2017.

[8] A. Krtschil, L. Orozco, S. Bechert, H. J. Wagner, F. Amtsberg, T.-y. Chen, A. Shah, A. Menges, and J. Knippers. "Structural development of a novel punctually supported timber building system for multi-storey construction." In: *Journal of Building Engineering* 58.March (2022), p. 104972. ISSN: 23527102. DOI: 10.1016/j.jobe.2022.104972.

[9] K. A. Malo, R. B. Abrahamsen, and M. A. Bjertnæs. "Some structural design issues of the 14-storey timber framed building "Treet" in Norway." In: *European Journal of Wood and Wood Products* 74.3 (2016), pp. 407–424. DOI: 10.1007/s00107-016-1022-5.

[10] B. Maurer, R. Maderebner, P. Zingerle, I. Färberböck, and M. Flach. "Point-Supported Flat Slabs with CLT-Panels." In: *Proc. of the World Conference on Timber Engineering (WCTE 2018)*. Seoul, Republic of Korea, 2018.

[11] M. Muster and A. Frangi. "Experimental analysis and structural modelling of the punching behaviour of continuous two-way CLT flat slabs." In: *Engineering Structures* 205 (2020), p. 110046. DOI: 10.1016/j.engstruct.2019.110046.

[12] L. Orozco, A. Krtschil, L. Skoury, J. Knippers, and A. Menges. "Arrangement of reinforcement in variable density timber slab systems for multi-story construction." In: *International Journal of Architectural Computing* 20.4 (2022), pp. 707–727. DOI: 10.1177/14780771221135003.

[13] L. Orozco, A. Krtschil, H. J. Wagner, S. Bechert, F. Amtsberg, L. Skoury, J. Knippers, and A. Menges. "Design Methods for Variable Density, Multi-Directional Composite Timber Slab Systems for Multi-Storey Construction." In: *Proc. of the 39th eCAADe Conference*. Novi Sad (SRB), 2021.

[14] M. Popovski, Z. Chen, and B. Gafner. "Structural behaviour of point-supported CLT floor systems." In: *Proc. of the World Conference on Timber Engineering (WCTE 2016)*. Vienna, Austria: Vienna University of Technology, 2016.

[15] L. Skoury, F. Amtsberg, X. Yang, H. J. Wagner, T. Wortmann, and A. Menges. "A Framework for managing data in multi-actor fabrication processes." In: *Design Modelling Symposium - Towards Radical Regeneration*. Berlin: Springer International Publishing, 2022. DOI: 10.1007/978-3-031-13249-0_47.

[16] H. Svatoš-Ražnjević, L. Orozco, and A. Menges. "Advanced Timber Construction Industry: A Review of 350 Multi-Storey Timber Projects from 2000–2021." In: *Buildings* 12.4 (2022), p. 404. DOI: 10.3390/buildings12040404.

[17] C. Tapia, M. Claus, and S. Aicher. "A finger-joint based LVL connection for the weak direction of CLT plates." In: *Construction and Building Materials* (2022). (accepted for publication).

[18] C. Tapia, L. Stimpfle, and S. Aicher. "A scalable column-CLT-slab connection for open-plan high-rise timber buildings." In: *Proc. of the World Conference on Timber Engineering (WCTE 2021)*. Santiago, Chile: Centro UC de Innovación en Madera, 2021.

[19] C. Tapia. *Pybaqus: A Python library for the visualization and post-processing of Abaqus ASCII result files*. Version 0.2.9. 2023. URL: https://github.com/cristobaltapia/pybaqus.

[20] C. Tapia. *Replication Data for: Point-support reinforcement for a highly efficient timber hollow core slab system*. Version V1. 2023. DOI: 10.18419/darus-3381.

[21] Z-9.1-775. *Technical Approval, Brettschichtholz mit dem Keilstoß-System "Hess Limiteless" für tragende Holzkonstruktionen – Approval holder: Hasslacher Holding GmbH*. Berlin, Germany: issued by Deutsches Institut für Bautechnik, 2020.

[22] S. Zöllig, A. Frangi, S. Franke, and M. Muster. "Timber structures 3.0 - new technology for multi-axial, slim, high performance timber structures." In: *Proc. of the World Conference on Timber Engineering (WCTE 2016)*. Vienna, Austria: Vienna University of Technology, 2016.